Frontiers in Heat and Mass Transfer (FHMT), 19, 36 (2022)
DOI: 10.5098/hmt.19.36

Global Digital Central
ISSN: 2151-8629

Frontiers in Heat and Mass Transfer

Available at www.ThermalFluidsCentral.org

IMPACT OF CHEMICAL REACTION, SORET NUMBER AND HEAT SOURCE ON UNSTEADY MHD CASSON FLUID FLOW PAST VERTICAL SURFACE

K.V. Chandra Sekhar*

Department of engineering Mathematics, College of Engineering, Koneru Lakshmaiah Education Foundation, Vaddeswaram, Guntur, Andhra Pradesh, India

ABSTRACT

The current study explores heat and mass transfer analysis of unstable MHD boundary layer flow of electrically conducting Casson fluid near an infinite Perpendicular porous plate, moving with variable velocity. Mass diffusion equation was described by the homogenous first order chemical reaction. The equations controlling the flow converted into dimensionless form and solved by applying Laplace transform method and the expressions for velocity, temperature and concentration of the flow are acquired in exact form. To understand the physical insight of the problem a detailed study of involved parameters of the flow was done and explained in detailed with graphs. The physical parameters of engineering interest are skin friction, Nussselt number and Sherwood number. The analytical expressions are procured in exact form in terms of error and exponential functions. The impact of different physical parameters is analyzed with the aid of the tables.

Keywords: Unsteady, MHD, Casson fluid, chemical reaction, Soret number, heat source, vertical surface.

1. INTRODUCTION

The role of porous media is quite significant in numerous energy and environmental system. That is why good number of authors done significant research work in heat transfer flows through porous media. An analytical study was done by Rapits and Perdikis (2004) on transient convective flow in a huge penetrable medium. Ghosh and Bég (2008) performed analytical survey on transient radiative - convective heat exchange in an identical, uniform permeable region beside a heated perpendicular plate. The result of chemical reaction on Convective heat and mass diffusion rates is quite significant. The effect will depend up on type of reaction heterogeneous or homogeneous.

An nth order chemical reaction is one where the rate of change is correlated with nth power of the reaction. Particularly if n is one it is a first order reaction. Occurrence of uncontaminated air or water is not possible, due to the presence of foreign mass either naturally or combined with air or water. This leads to chemical reaction. The investigation of such chemical reaction is helpful in developing some food products and production polymers. Cussler (1998). Chambre and Young (1958) exposed first order toxic and creative chemical reaction problems near a horizontal plate. Uniform chemical reaction of first order effects on the flow past an impulsively moving infinite vertical plate with invariable heat and mass transfer was analyzed by Das et al. (1994). Nield, D.A, Bejan, A(1999), Postelnicu A (2007) and Prased KV et al.(2003) gone through effects of chemical reaction of various flows in porous media. Mohamed et.al (2013) analyzed unstable Magneto hydrodynamic double-diffusive convective boundary layer flow above radiate heated vertical surface in an isotropous, analogous penetrable regime with chemical reaction and heat sink. Due to their enormous applications in process of plastic sheets, glass fiber production, recently the study of non-Newtonian fluids has got good attention of the researchers.

Casson fluid is a non-Newtonian fluid, which has vast applications in industries of polymers and biomechanics. Casson fluid is a shear thinning liquid having infinite viscosity at zero of shear and yield stess under which no flow occurs and zero viscosity at infinite rate of shear. It is a key model used in many food stuffs and biological materials like blood, which narrates steady shear stress, steady shear rate behavior of blood. Kataria et al.(2016) done a deep study on Soret and heat generation effects on MHD Casson fluid flow. Sulochana, C and Poornima M (2019) investigated Casson fluid flow through perpendicular plate in companionship of hall current. Vijaya et al (2020) explore binary chemical reaction along with activation energy of an electrically conducting incompressible Casson fluid induced due to stretching surface. In addition, Vijaya et al. (2021) investigated the effect of thermophoresis, buoyancy effects combined with chemical reaction and magnetic effects on Maxwell fluid over a surface with exponentially stretching sheet. Later Talha Anwar et al. (2021) and Haroon et al. (2022) have studied the MHD casson fluid flow under the influence of different physical parameters.

In the above survey the vertical plate moving with variable velocity under Soret effect was ignored. The present analysis is extension of Mohamed, R.A et al. (2013) focusing on MHD casson fluid flow with variable velocity and Soret effect. The governing equations are converted as dimensionless using dimensionless parameters and solved using the method of Laplace transforms. Velocity, temperature and concentration of species behave accordingly under the control of different physical parameters. These things are discussed in detailed.

2. MATHEMATICAL CONFIGURATION

A two-dimensional, unstable laminar flow of viscous, electrically conducting incompressible fluid with heat source past a semi-infinite vertical plate moving with changeable velocity immersed in medium with porousnes. The $\tilde{x}$ axis is considered in the direction of perpendicular plate in the upside direction and $\tilde{y}$ axis is considered perpendicular to the plate. At $\tilde{t} \leq 0$, the fluid and the plate are having equal temperatures T and concentrations C. At time $\tilde{t} > 0$, the plate moves with variable velocity $U\tilde{t}$ in the upside direction. Invariable

* Corresponding author E-mail: kasulanati22@rediffmail.com

DOI: 10.5098/hmt.19.36
ISSN: 2151-8629

magnetic field is enforced perpendicular to the plate. Produced magnetic field was ignored as magnetic Reynolds number and applied voltage are assumed to be very small. All fluid characteristics are considered invariable excluding the impact of density variation with temperature and concentration. Gravitational force acts in opposite line to the right side of $\tilde{x}$ axis. A chemical reaction of first order is considered among fluid and species concentration uniformly. The Hall effects, Joule heating viscous dissipation are ignored. The flow phenomena illustrated in fig – 1.

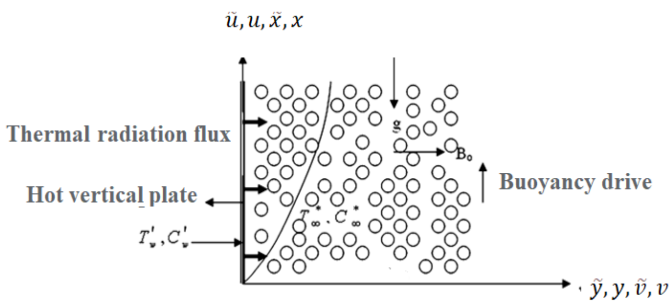

Fig-1: Outline of the phenomena

The equations describing the flow are as given under

$$\frac{\partial \tilde{u}}{\partial \tilde{t}} = \nu\left(1+\frac{1}{\beta}\right)\frac{\partial^2 \tilde{u}}{\partial \tilde{y}^2} - \frac{\sigma B_0{}^2 \tilde{u}}{\rho} + g\tilde{\beta}\left(\tilde{T}-\tilde{T}_\infty\right) + g\beta\left(\tilde{C}-\tilde{C}_\infty\right) - \frac{\nu}{k}\tilde{u} \tag{1}$$

$$\frac{\partial \tilde{T}}{\partial \tilde{t}} = \frac{\kappa}{\rho c_p}\frac{\partial^2 \tilde{T}}{\partial \tilde{y}^2} - \frac{Q_0}{\rho c_p}\left(\tilde{T}-\tilde{T}_\infty\right) - \frac{1}{\rho c_p}\frac{\partial q_r}{\partial \tilde{y}} \tag{2}$$

$$\frac{\partial \tilde{C}}{\partial \tilde{t}} = D_M\frac{\partial^2 \tilde{C}}{\partial \tilde{y}^2} + \frac{D_M k_T}{T_M}\frac{\partial^2 \tilde{T}}{\partial \tilde{y}^2} - k\tilde{r}\left(\tilde{C}-\tilde{C}_\infty\right) \tag{3}$$

$$\begin{aligned} &\tilde{u}=0, \tilde{T}=\tilde{T}_\infty, \tilde{C}=\tilde{C}_\infty \text{ for all } \tilde{y}\ge 0, \tilde{t}\le 0 \\ &\tilde{u}=U\tilde{t}, \tilde{T}=\tilde{T}_w, \tilde{C}=\tilde{C}_w \text{ at } \tilde{y}=0, \tilde{t}>0 \\ &\tilde{u}\to 0, \tilde{C}\to\tilde{C}_\infty, \tilde{T}\to\tilde{T}_\infty \text{ as } \tilde{y}\to\infty, \tilde{t}>0 \end{aligned} \tag{4}$$

$$\theta = \frac{\tilde{T}-\tilde{T}_\infty}{\tilde{T}_w-\tilde{T}_\infty}, \phi = \frac{\tilde{C}-\tilde{C}_\infty}{\tilde{C}_w-\tilde{C}_\infty}, \ u=\frac{\tilde{u}}{U_0}, y=\frac{\tilde{y}U_0}{\nu}, t=\frac{\tilde{t}U^2{}_0}{\nu},$$

$$Gr = \frac{\nu g\beta\left(\tilde{T}_w-\tilde{T}_\infty\right)}{U_0{}^3}, \ Gm = \frac{\nu g\tilde{\beta}\left(\tilde{C}_w-\tilde{C}_\infty\right)}{U_0{}^3}, \mathbf{Pr} = \frac{\mu c_p}{\kappa} = \frac{\nu\rho c_p}{\kappa}$$

$$Sc = \frac{\nu}{D_M}, \ M^2 = \frac{\sigma B_0{}^2\nu}{\rho U_0{}^2}, \ Sr = \frac{D_M k_T\left(\tilde{T}_w-\tilde{T}_\infty\right)}{\nu T_M\left(\tilde{C}_w-\tilde{C}_\infty\right)} \tag{5}$$

$$Q = \frac{Q_0\nu^2}{\rho c_p U_0{}^2}, \ k_p{}^2 = \frac{\nu^2}{kU_0{}^2}$$

Using non- dimensional variables (5), equations (1),(2) and (3) becomes

$$\frac{\partial u}{\partial t} = \frac{\partial^2 u}{\partial y^2} - \left(M^2 + k_p{}^2\right)u + Gr\theta + Gm\phi \tag{6}$$

$$\frac{\partial \theta}{\partial t} = (1+R)(Pr)^{-1}\frac{\partial^2 \theta}{\partial y^2} - Q\theta \tag{7}$$

$$\frac{\partial \phi}{\partial t} = (Sc)^{-1}\frac{\partial^2 \phi}{\partial y^2} + Sr\frac{\partial^2 \theta}{\partial y^2} - kr\phi \tag{8}$$

The boundary conditions (4) transformed are as given below

$$\begin{aligned} &u=0, \theta=0, \phi=0 \text{ for all } y\ge 0, t\le 0 \\ &u=t, \theta=1, \phi=1 \text{ at } y=0, t>0 \\ &u\to 0, \theta\to 0, \phi\to 0 \text{ as } y\to\infty, t>0 \end{aligned} \tag{9}$$

3. ANALYTICAL SOLUTION THROUGH LAPLACE TRANSFORM

Employing Laplace transform to the equations (6) to (8) using conditions (9), we get Ordinary differential equations

$$\frac{d^2u}{dy^2} - B_3\left(B_4+s\right)u = -B_3\left(Gr\theta(y,s) + Gm\phi(y,s)\right) \tag{10}$$

$$\frac{d^2\theta}{dy^2} - \frac{Pr}{1+R}(s+Q)\theta(y,s) = 0 \tag{11}$$

$$\frac{d^2\phi}{dy^2} - Sc(s+kr)\phi(y,s) = -ScSr\frac{Pr}{1+R}(s+Q)\theta(y,s) \tag{12}$$

Solving the above equations (10) to (12), we get

$$\begin{aligned} u(y,s) = &\left\{\frac{1}{s^2} + \frac{A_{15}}{s(s+A_{14})} + \frac{(1-A_8)Gm}{A_{19}s(s+A_{21})} - \frac{A_8Gm}{A_{20}s(s+A_{22})} - \frac{A_9Gm}{A_{19}(s+A_5)(s+A_{22})}\right\}e^{-y\sqrt{B_4+s}} \\ &- \frac{A_{15}}{s(s+A_{14})}e^{-y\sqrt{B_5}\sqrt{s+Q_0}} + \frac{(-1+A_8)Gm}{A_{19}s(s+A_{21})}e^{-y\sqrt{Sc}\sqrt{s+kr}} \\ &+ \frac{A_8Gm}{A_{20}s(s+A_{22})}e^{-y\sqrt{B_5}\sqrt{s+Q_0}} \\ &+ \frac{A_9Gm}{A_{19}(s+A_5)(s+A_{22})}e^{-y\sqrt{Sc}\sqrt{s+kr}} \\ &- \frac{A_9Gm}{A_{19}(s+A_5)(s+A_{22})}e^{-y\sqrt{B_5}\sqrt{s+Q_0}} \end{aligned} \tag{13}$$

$$\theta(y,s) = \frac{1}{s}e^{-y\sqrt{B_5}\sqrt{s+Q}} \tag{14}$$

$$\phi(y,s) = \left(\frac{1}{s} - \frac{A_8}{s} - \frac{A_9}{s+A_5}\right)e^{-y\sqrt{sc}\sqrt{s+kr}} + \left(\frac{A_8}{s} + \frac{A_9}{s+A_5}\right)e^{-y\sqrt{B_5}\sqrt{s+Q_0}} \tag{15}$$

Applying inverse Laplace transform for the equations (13) to (15)

$$\begin{aligned} u(y,t) = &\frac{1}{2}\left\{\left(t - \frac{y}{2\sqrt{B_4}}\right)e^{-y\sqrt{B_3}\sqrt{B_4}}\operatorname{erfc}\left(y\sqrt{B_3}\left(2\sqrt{t}\right)^{-1} - \sqrt{B_4t}\right) + \left(t + \frac{y}{2M}\right)e^{-y\sqrt{B_3}\sqrt{B_4}}\operatorname{erfc}\left(y\sqrt{B_3}\left(2\sqrt{t}\right)^{-1} + \sqrt{B_4t}\right)\right\} \\ &+ A_{16}\left[\left\{e^{-y\sqrt{B_3}\sqrt{B_4}+B_4t}\operatorname{erfc}\left(y\sqrt{B_3}\left(2\sqrt{t}\right)^{-1} - \sqrt{B_4t}\right) + e^{y\sqrt{B_3}\sqrt{B_4}+B_4t}\operatorname{erfc}\left(y\sqrt{B_3}\left(2\sqrt{t}\right)^{-1} + \sqrt{B_4t}\right)\right\}\right. \\ &- \left\{e^{-y\sqrt{B_3}\sqrt{A_{14}-B_4}+(A_{14}-B_4)t}\operatorname{erfc}\left(y\sqrt{B_3}\left(2\sqrt{t}\right)^{-1} - M\sqrt{(A_{14}-B_4)t}\right)\right. \\ &\left.\left.- e^{y\sqrt{B_3}\sqrt{A_{14}-B_4}+(A_{14}-B_4)t}\operatorname{erfc}\left(y\sqrt{B_3}\left(2\sqrt{t}\right)^{-1} + M\sqrt{(A_{14}-B_4)t}\right)\right\}\right] \\ &\frac{(1-A_8)Gm}{A_{19}A_{21}}\left\{\left[e^{-y\sqrt{B_3}\sqrt{B_4}+B_4t}\operatorname{erfc}\left(y\sqrt{B_3}\left(2\sqrt{t}\right)^{-1} - \sqrt{B_4t}\right)\right.\right. \\ &\left.+ e^{-y\sqrt{B_4}+B_4t}\operatorname{erfc}\left(y\sqrt{B_3}\left(2\sqrt{t}\right)^{-1} - \sqrt{B_4t}\right)\right] \end{aligned} \tag{16}$$

DOI: 10.5098/hmt.19.36

ISSN: 2151-8629

$$-\Big[e^{-y\sqrt{B_3}\sqrt{A_{14}-B_4}+(A_{14}-B_4)t}\operatorname{erfc}\left(\frac{y\sqrt{B_3}}{2\sqrt{t}}-M\sqrt{(A_{14}-B_4)t}\right)$$

$$+e^{y\sqrt{B_3}\sqrt{A_{14}-B_4}+(A_{14}-B_4)t}\operatorname{erfc}\left(\frac{y\sqrt{B_3}}{2\sqrt{t}}+M\sqrt{(A_{14}-B_4)t}\right)\Big]\Big]\Big\}$$

$$-\frac{A_8Gm}{A_{20}A_{22}}\left\{\begin{array}{l}\Big[e^{-y\sqrt{B_4}+B_4t}\operatorname{erfc}\left(\frac{y\sqrt{B_3}}{2\sqrt{t}}-B_4\sqrt{t}\right)\\ +e^{y\sqrt{B_4}+B_4t}\operatorname{erfc}\left(\frac{y\sqrt{B_3}}{2\sqrt{t}}+B_4\sqrt{t}\right)\Big]\end{array}\right.$$

$$\Big[e^{-y\sqrt{A_{22}-B_4}+(A_{22}-B_4)t}\operatorname{erfc}\left(\frac{y\sqrt{B_3}}{2\sqrt{t}}-M\sqrt{(A_{22}-B_4)t}\right)$$

$$+e^{y\sqrt{A_{22}-B_4}+(A_{22}-B_4)t}\operatorname{erfc}\left(\frac{y}{2\sqrt{t}}+M\sqrt{(A_{22}-B_4)t}\right)\Big]\Big]\Big\}$$

$$-\frac{A_9Gm}{A_{19}(A_5-A_{21})}\Big[\Big[e^{-y\sqrt{B_3}\sqrt{A_5-B_4}+(A_5-B_4)t}\operatorname{erfc}\left(\frac{y\sqrt{B_3}}{2\sqrt{t}}-M\sqrt{(A_5-B_4)t}\right)$$

$$+e^{y\sqrt{B_3}\sqrt{A_5-B_4}+(A_5-B_4)t}\operatorname{erfc}\left(y\sqrt{B_3}+M\sqrt{(A_5-B_4)t}\right)\Big]$$

$$\Big[e^{-y\sqrt{A_{21}-B_4}+(A_{21}-B_4)t}\operatorname{erfc}\left(\frac{y\sqrt{B_3}}{2\sqrt{t}}-M\sqrt{(A_{21}-B_4)t}\right)$$

$$+e^{y\sqrt{A_{21}-M^2}+(A_{21}-M^2)t}\operatorname{erfc}\left(\frac{y\sqrt{B_3}}{2\sqrt{t}}+M\sqrt{(A_{21}-B_4)t}\right)\Big]\Big]$$

$$+\frac{A_9Gm}{A20(A_5-A_{22})}\Big\{\Big[e^{-y\sqrt{B_3}\sqrt{A_5-B_4}+(A_5-B_4)t}\operatorname{erfc}\left(\frac{y\sqrt{B_3}}{2\sqrt{t}}-\sqrt{B_4}\sqrt{(A_5-B_4)t}\right)$$

$$+e^{y\sqrt{B_3}\sqrt{A_5-B_4}+(A_5-M^2)t}\operatorname{erfc}\left(\frac{y\sqrt{B_3}}{2\sqrt{t}}+\sqrt{B_4}\sqrt{(A_5-B_4)t}\right)\Big]$$

$$-\Big[e^{-y\sqrt{B_3}\sqrt{A_{22}-B_4}+(A_{22}-B_4)t}\operatorname{erfc}\left(\frac{y\sqrt{B_3}}{2\sqrt{t}}-\sqrt{B_4}\sqrt{B_4t}\right)$$

$$+e^{y\sqrt{B_3}\sqrt{A_{22}-B_4}+(A_{22}-B_4)t}\operatorname{erfc}\left(\frac{y\sqrt{B_3}}{2\sqrt{t}}+\sqrt{B_4}\sqrt{(A_{22}-B_4)t}\right)\Big]\Big\}$$

$$-\frac{A_{16}}{A_{14}}\Big[\Big[e^{-y\sqrt{B_5Q}+Qt}\operatorname{erfc}\left(\frac{y\sqrt{B_5}}{2\sqrt{t}}-\sqrt{Qt}\right)$$

$$+e^{y\sqrt{B_5Q}+Qt}\operatorname{erfc}\left(\frac{y\sqrt{B_5}}{2\sqrt{t}}+\sqrt{Qt}\right)\Big]$$

$$-\Big[e^{-y\sqrt{A_{14}-Q}+(A_{14}-Q)t}\operatorname{erfc}\left(\frac{y}{2\sqrt{t}}-B_4\sqrt{(A_{14}-Q)t}\right)$$

$$+e^{y\sqrt{A_{14}-Q}+(A_{22}-B_4)t}\operatorname{erfc}\left(\frac{y}{2\sqrt{t}}+B_4\sqrt{(A_{14}-Q)t}\right)\Big]\Big]$$

$$+\frac{(-1+A_8)Gm}{A_{19}A_{21}}\Big[e^{-y\sqrt{Sckr}+krt}\operatorname{erfc}\left(y\sqrt{Sc}(2\sqrt{t})^{-1}-\sqrt{krt}\right)$$

$$+e^{y\sqrt{Sckr}+krt}\operatorname{erfc}\left(y\sqrt{Sc}(2\sqrt{t})^{-1}+\sqrt{krt}\right)\Big]$$

$$\Big[e^{-y\sqrt{Sc(A_{21}-kr)}+(A_{21}-kr)t}\operatorname{erfc}\left(\frac{y}{2\sqrt{t}}-M\sqrt{(A_{21}-kr)t}\right)$$

$$+e^{y\sqrt{Sc(A_{21}-kr)}+(A_{21}-kr)t}\operatorname{erfc}\left(\frac{y}{2\sqrt{t}}+M\sqrt{(A_{21}-kr)t}\right)\Big]$$

$$e^{-y\sqrt{Sckr}+krt}\operatorname{erfc}\left(y\sqrt{Sc}(2\sqrt{t})^{-1}-\sqrt{krt}\right)$$

$$+\frac{A_9Gm}{A_{19}(A_5-A_{22})}$$

$$\times\Big[e^{-y\sqrt{\mathbf{Sc}(A_5-kr)}+(A_5-kr)t}\operatorname{erfc}\left(y\sqrt{\mathbf{Sc}}(2\sqrt{t})^{-1}-\sqrt{(A_5-kr)t}\right)$$

$$+e^{y\sqrt{\mathbf{Sc}(A_5-kr)}+(A_5-kr)t}\operatorname{erfc}\left(y\sqrt{\mathbf{Sc}}(2\sqrt{t})^{-1}+\sqrt{(A_5-kr)t}\right)$$

$$-\Big[e^{-y\sqrt{\mathbf{Pr}(A_{21}-kr)}+(A_{21}-kr)t}\operatorname{erfc}\left(y(2\sqrt{t})^{-1}-M\sqrt{\begin{pmatrix}A_{21}\\-kr\end{pmatrix}t}\right)$$

$$+e^{y\sqrt{\mathbf{Pr}(A_{21}-kr)}+(A_{21}-kr)t}\operatorname{erfc}\left(y(2\sqrt{t})^{-1}+M\sqrt{(A_{21}-kr)t}\right)\Big]\Big]$$

$$+\frac{A_9Gm}{A_{19}(A_5-A_{22})}$$

$$\times\Big\{\Big[e^{-y\sqrt{B_5(A_5-Q)}+(A_5-Q)t}\operatorname{erfc}\left(\frac{y\sqrt{\mathbf{Sc}}}{2\sqrt{t}}-\sqrt{(A_5-Q)t}\right)$$

$$+e^{y\sqrt{B_5(A_5-Q)}+(A_5-Q)t}\operatorname{erfc}\left(\frac{y\sqrt{\mathbf{Sc}}}{2\sqrt{t}}+\sqrt{(A_5-Q)t}\right)\Big]$$

$$+\frac{A_9Gm}{A_{19}(A_5-A_{22})}\Big\{\Big[e^{-y\sqrt{B_5(A_5-Q)}+(A_5-Q)t}\operatorname{erfc}\left(\frac{y\sqrt{\mathbf{Sc}}}{2\sqrt{t}}-\sqrt{(A_5-Q)t}\right)$$

$$+e^{y\sqrt{B_5(A_5-Q)}+(A_5-Q)t}\operatorname{erfc}\left(\frac{y\sqrt{\mathbf{Sc}}}{2\sqrt{t}}+\sqrt{(A_5-Q)t}\right)\Big]$$

$$-\Big[e^{-y\sqrt{B_5(A_{22}-Q)}+(A_{22}-Q)t}\operatorname{erfc}\left(\frac{y}{2\sqrt{t}}-\sqrt{B_4}\sqrt{(A_{22}-Q)t}\right)$$

$$++e^{y\sqrt{B_5(A_{22}-Q)}+(A_{22}-Q)t}\operatorname{erfc}\left(\frac{y}{2\sqrt{t}}+B_4\sqrt{(A_{22}-Q)t}\right)\Big]\Big]\Big\} \qquad (16)$$

$$\theta(y,t)=\frac{1}{2}\left\{\begin{array}{l}e^{-y\sqrt{B_5Q}+Q_0t}\operatorname{erfc}\left(y\sqrt{B_5}(2\sqrt{t})^{-1}-\sqrt{Qt}\right)\\ +e^{y\sqrt{B_5Q}+Qt}\operatorname{erfc}\left(y\sqrt{B_5}(2\sqrt{t})^{-1}+\sqrt{Qt}\right)\end{array}\right\} \qquad (17)$$

$$\phi(y,t)=\frac{(1-A_8)}{2}\left\{\begin{array}{l}\Big[\Big[e^{-y\sqrt{Sckr}+krt}\operatorname{erfc}\left(\frac{y\sqrt{Sc}}{2\sqrt{t}}-\sqrt{krt}\right)\\ +e^{y\sqrt{Sckr}+krt}\operatorname{erfc}\left(\frac{y\sqrt{Sc}}{2\sqrt{t}}+\sqrt{krt}\right)\Big]\Big]\end{array}\right\}$$

$$+\frac{A_9}{2}\Big[e^{-y\sqrt{B_5(A_5-Q)}+(A_5-Q)t}\operatorname{erfc}\left(y\sqrt{B_5}(2\sqrt{t})^{-1}-\sqrt{(A_5-Q)t}\right)$$

$$+e^{y\sqrt{B_5(A_5-Q)}+(A_5-Q)t}\operatorname{erfc}\left(y\sqrt{B_5}(2\sqrt{t})^{-1}+\sqrt{(A_5-Q)t}\right)\Big]$$

$$\Big[e^{-y\sqrt{Sc(A_5-kr)}+(A_5-kr)t}\operatorname{erfc}\left(\frac{ySc}{2\sqrt{t}}-\sqrt{(A_5-kr)t}\right)$$

DOI: 10.5098/hmt.19.36

ISSN: 2151-8629

$$+e^{y\sqrt{Sc(A_5-kr)}+(A_5-kr)t}\operatorname{erfc}\left(\frac{ySc}{2\sqrt{t}}+\sqrt{(A_5-kr)t}\right)\Bigg]$$

$$+\frac{A_8}{2}\left\{\begin{array}{l} e^{-y\sqrt{B_5Q}+Q_0t}\operatorname{erfc}\left(y\sqrt{B_5}\left(2\sqrt{t}\right)^{-1}-\sqrt{Qt}\right) \\ +e^{y\sqrt{B_5Q}+Qt}\operatorname{erfc}\left(y\sqrt{B_5}\left(2\sqrt{t}\right)^{-1}+\sqrt{Qt}\right)\end{array}\right\} \tag{18}$$

The expressions for shear stress (velocity gradient), temperature gradient and concentration gradient are presented here under Eq. (19).

$$-\left(1+\frac{1}{\beta}\right)\frac{\partial u}{\partial y}\bigg|_{y=0}$$
$$=\left(-A_{16}+\frac{1-A_8}{A_{19}A_{21}}-\frac{A_8Gm}{A_{20}A_{22}}\right)\left(\sqrt{B_4}e^{-B_4t}\operatorname{erf}\left(\sqrt{B_4}\sqrt{t}\right)+\frac{e^{-B_4t}}{\sqrt{\pi t}}\right)$$
$$+\left(\frac{A_8-1}{A_{19}A_{21}}-\frac{A_9Gm}{A_{19}(A_5-A_{21})}\right)(B_4-A_{21})\left(\begin{array}{l}\frac{1}{\sqrt{A_{21}-B_4}}e^{(A_{21}-B_4)t} \\ +\operatorname{erf}\left(\sqrt{(A_{21}-B_4)t}\right)+\frac{e^{-B_4t}}{\sqrt{\pi t}}\end{array}\right)$$
$$+\left(\frac{A_8Gm}{A_{20}A_{22}}+\frac{A_9Gm}{A_{20}(A_5-A_{22})}\right)(B_4-A_{22})\left(\begin{array}{l}\frac{1}{\sqrt{A_{22}-B_4}}e^{(A_{22}-B_4)t} \\ +\operatorname{erf}\left(\sqrt{(A_{22}-B_4)t}\right)+\frac{e^{-B_4t}}{\sqrt{\pi t}}\end{array}\right)$$
$$+\left(\frac{A_9Gm}{A_{19}(A_5-A_{21})}-\frac{A_9Gm}{A_{20}(A_5-A_{22})}\right)\times(B_4-A_{22})$$
$$\times\left(\frac{1}{\sqrt{A_5-M^2}}e^{(A_5-B_4)t}+\operatorname{erf}\left(\sqrt{(A_5-B_4)t}\right)+\frac{e^{-B_4t}}{\sqrt{\pi t}}\right)$$
$$+\left(\begin{array}{l}A_{16}\sqrt{B_5} \\ -\frac{A_8Gm\sqrt{B_5}}{A_{20}A_{22}}\end{array}\right)\left(\sqrt{Q}e^{-Qt}\operatorname{erf}\left(\sqrt{Qt}\right)+\frac{e^{-Qt}}{\sqrt{\pi t}}\right) \tag{19}$$

$$\frac{\partial\theta}{\partial y}\bigg|_{y=0}=\frac{2}{\sqrt{\pi}}-e^{Qt}\sqrt{B_5Q} \tag{20}$$

$$\frac{\partial\phi}{\partial y}\bigg|_{y=0}=$$
$$(1-A_8)\left\{\sqrt{\frac{Sc}{t\pi}}e^{-krt}+\sqrt{Sc}e^{krt}\operatorname{erf}\left(\sqrt{krt}\right)\right\}-A_9Sc\sqrt{kr-A_5}e^{-A_5t} \tag{21}$$
$$+\sqrt{B_5}A_8\frac{1}{\sqrt{\pi t}}e^{-Qt}+\sqrt{Q}e^{Qt}\operatorname{erf}\sqrt{Qt}+\sqrt{B_5}A_9\frac{1}{\sqrt{\pi t}}e^{-Qt}$$
$$-\sqrt{A_5-Q}e^{(A_5-Q)t}\operatorname{erf}\left(\sqrt{(A_5-Q)t}\right)$$

4. RESULTS AND DISCUSSION

To understand the phenomena exactly, the effect of disimmilar critical parameters on the flow are explained graphically. In fig – 2 we can see the velocity profiles plotted for disimilar values of Casson parameter. Viscosity of the fluid rises due to grow in Casson parameter and hence decrement in velocity. Fig – 3 exhibits that velocity of the fluid escalates with rise in Gr. Thermal Grashof number is ratio of thermal buoyancy force to viscous hydrodynamic force. Impact of thermal buoyancy force is more effective in the companionship of free convection, which intensify fluid velocity. This is due to increase in thermal buoyancy. Fig -4 depicts impact of magnetic parameter on velocity profiles. Rise in magnetic parameter sustains a deacclerate effect over the velocity profiles. This is because rise in magnetic parameter produces lorenz forces which opposes fluid motion. Fig – 5 displays grow in prandtl number effects fall in fluid velocity. Prandtl number gives ratio of kinematic viscosity to heat dispersion. Rise in Prandtl number diminishes heat control and enhances fluid viscosity which results in rise in thickness of the fluid that results in decrement in velocity. Increase of pore size opposes the fluid motion and hence decrese in velocity of the fluid. This fact was illustrated in fig – 6. Fluid temperature declines with rise in Pr. The density of the thermal boundary layer anhances as there is a fall in Prandtl number and hence temperature profile falls down with increment in Prandtl number. This was shown in fig – 7. Figure – 8 shows, escalate of heat source parameter rises temperature of the fluid. Schmidt number gives the relative influence of momentum to the mass dissipation of species concentration, which gives a decline in concentration. Fig -9 shows that increase of radiation parameter results in increase of temperature of the fluid. This due to the fact that rise in the radiation variable upsurges the thermic outline layer thickness. Schmidt number gives the comparative influence of momentum to the mass diffusion of species concentration, which gives a decrement in concentration. This fact is shown fig- 10. From fig – 11 we can notice that Soret number effects raise in molecular dissipation and hence escalation in concentration of the fluid. Fig – 12 shows the impact of chemical reaction parameter on concentration profiles. When chemical reaction grows, dispensation of concentration dimnishes, which in turn results in escalation of transport phenomena and hence increment in concentration dispensation.

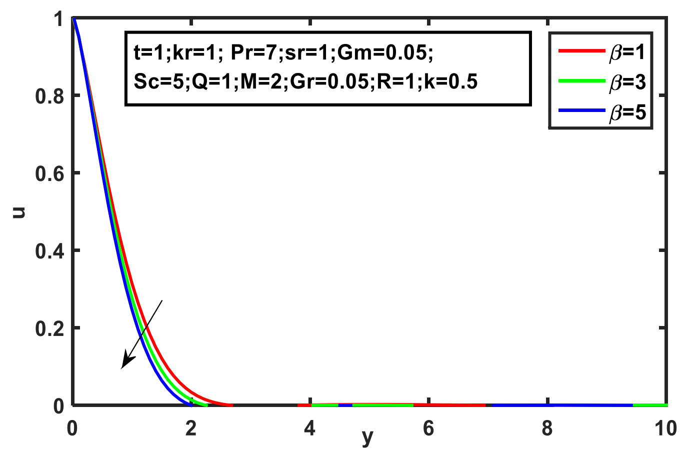

Fig. 2: Velocity outline versus Casson parameter β

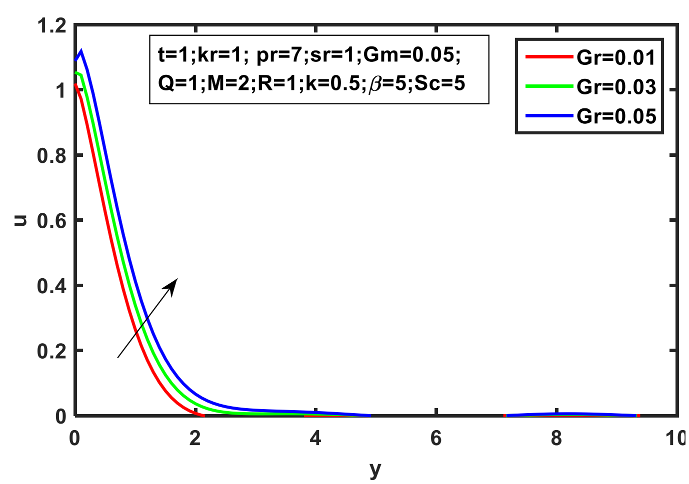

Fig. 3: Velocity outline for dissimilar values of Gr

Frontiers in Heat and Mass Transfer (FHMT), 19, 36 (2022)
DOI: 10.5098/hmt.19.36
Global Digital Central
ISSN: 2151-8629

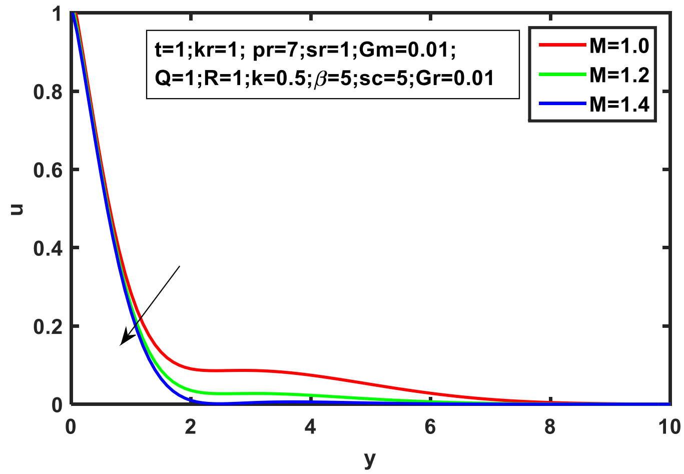

Fig. 4: Velocity outline for distinct values of M

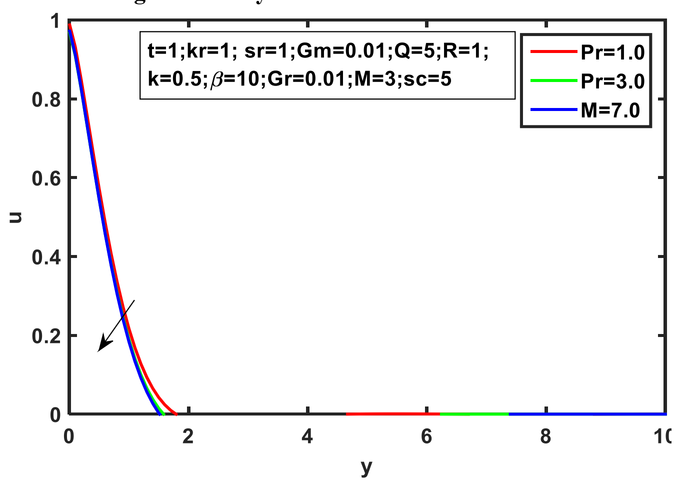

Fig. 5: Velocity outline for distinct values of Pr

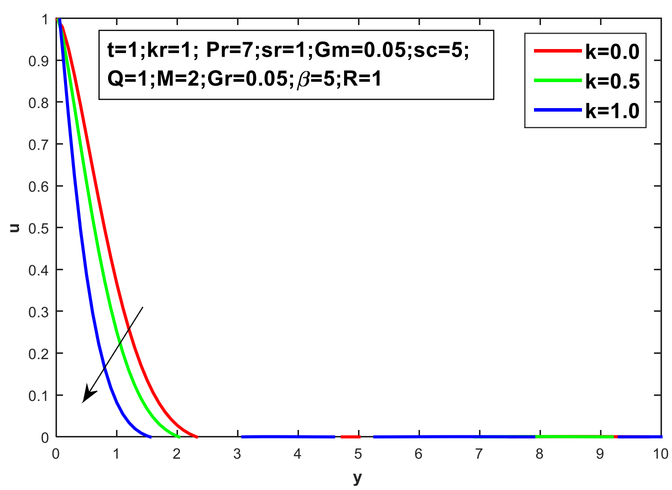

Fig. 6: Velocity outline versus permeability parameter k

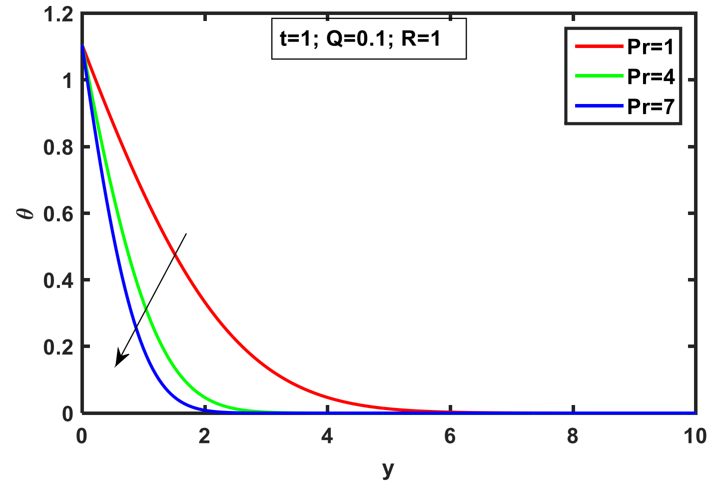

Fig. 7: Temperature outline for varying values of Pr

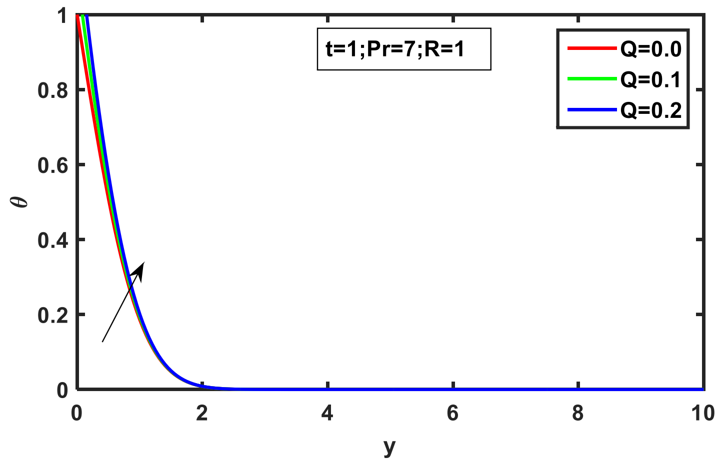

Fig. 8: Temperature versus heat source parameter Q

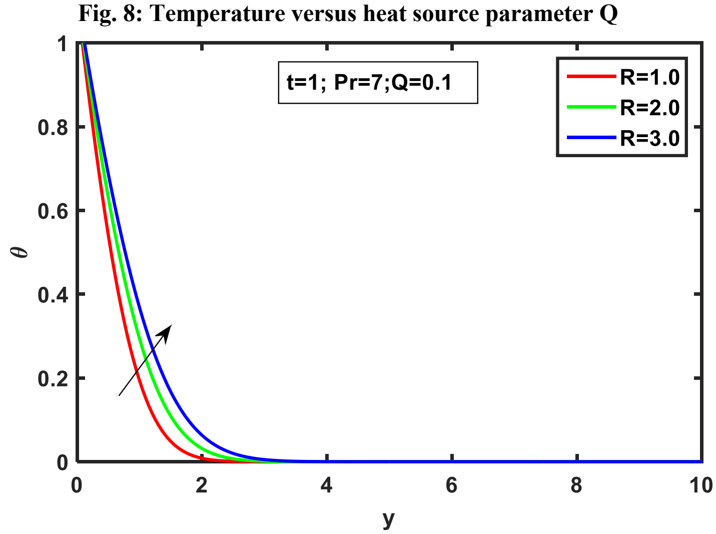

Fig. 9: Temperature outline under the influence of R

DOI: 10.5098/hmt.19.36
ISSN: 2151-8629

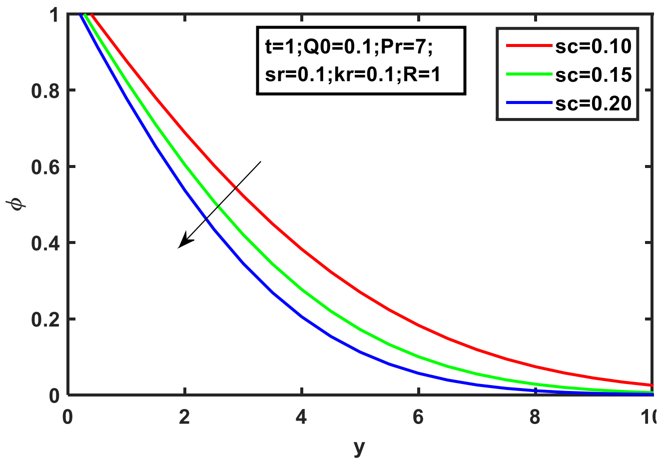

Fig. 10: Variation of Concentration profiles for unlike values of Sc

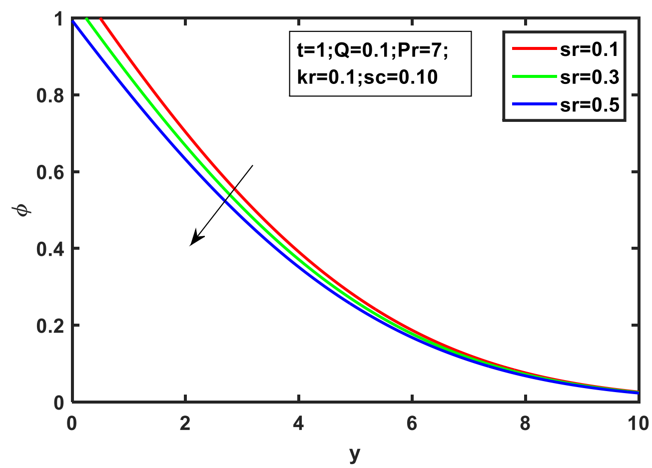

Fig. 11: Concentration outline for un identical values of sr

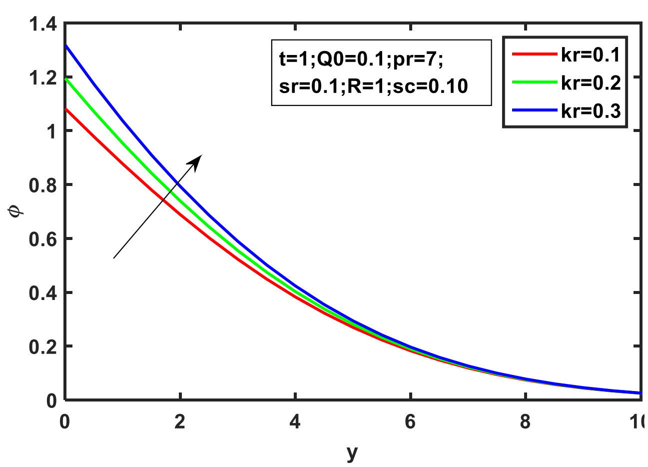

Fig. 12: Concentration outline for un identical values of kr

Moreover the variation of shear stress function, temperature gradient function and concentration gradient functions with reference to different physical parameters are presented in tables 1 2 and 3. The values are in good agreement with physical insight of the problem

Table 1: **Shear stress (velocity gradient) for distinct values of Gm, Gr, k, β ,M, Pr, Sc when** $Q=1, t=1, kr=1, sr=1$

Gm	Gr	k	β	M	Pr	Sc	$-\left(1+\frac{1}{\beta}\right)\frac{\partial u}{\partial y}\Big\vert_{y=0}$
0.01							0.109021
0.03							0.114950
0.05							0.118906
	0.01						0.068010
	0.03						0.098214
	0.05						0.107171
		0.0					0.181232
		0.5					0.192244
		1.0					0.175270
			1				0.068010
			2				0.098214
			3				0.115836
				1.0			0.082626
				1.2			0.104623
				1.4			0.111457
					1		0.070184
					2		0.095003
					7		0.102758
						0.05	0.120278
						0.10	0.111203
						1.15	0.111296

Table 2: Temperature gradient for disimillar values of Pr, Q, t **when t=1**

Pr	R	Q	$\frac{\partial \theta}{\partial y}\Big\vert_{y=0}$
1.0			-0.063550
4.0			-0.062408
7.0			-0.061094
	1		-0.045047
	2		-0.044502
	3		-0.043895
		0.0	-0.075854
		0.1	-0.073618
		0.2	-0.071285

Table 3: Concentration gradient for distinct values of Sc, kr and Sr when $Pr=7, Q=0.1$, t=1

kr	Sc	Sr	$\frac{\partial \phi}{\partial y}\Big\vert_{y=0}$
0.1			-0.115265
0.3			-0.094376
0.5			-0.084156
	0.10		-0.143616
	0.15		-0.136076
	0.20		-0.126468
		0.3	0.030308
		0.5	0.022052
		0.7	0.014838

4 NOMENCLATURE

t	Non dimensional time
$\tilde{t}$	dimensional time
$\tilde{T}$	temperature of the fluid
$\tilde{T}_w, \tilde{C}_w$	Temperature and concentration of the surface
$\tilde{T}_\infty$	Free stream temperature
u	Non dimensional velocity
U	Plate velocity in motion
$\tilde{u}, \tilde{v}$	Parts of dimensional velocities along Coordinate axis
$\tilde{x}, \tilde{y}$	Plate Dimensional distances along coordinate axis
y	Dimensionless distance
β	Thermal expansion factor
$\tilde{\beta}$	Factor of diffusion with concentration
θ	dimensionless temperature
ν	diffusivity of momentum
ρ	Density of the fluid
σ	electrical conductivity of the fluid
Q_0	Production/assimilation of heat
$\tilde{k}_r$	Chemical reaction rate of first order
Sc	Schmidt number
β	Casson parameter
$\bar{\sigma}$	Stefan-Boltzmann flux
ϕ	Non dimensional concentration
sr	Soret number
R	Radiation Parameter
B_0	Induction of Magnetic field
$\tilde{C}$	Fluid concentration
$\tilde{C}_\infty$	Free stream concentration of the fluid
c_p	specific heat at constant pressure
D	coefficient of diffusion effectiveness
g	Acceleration due to gravity
Gc	Solutal Grashof number
Gr	Grashof number
k	Permeableness of the porous medium
$\tilde{K}$	coefficient of Spectral mean absorption
k_1	Thermal conductivity parameter
k_r	parameter of thermal radiation conduction
k^2	Porousness parameter
M	Parameter of magnetized field
Pr	Prandtl number
q_r	Heat flux due to radiation

5 REFERENCES

Sulochana, C and Poornima, M Unsteady MHD Casson fluid flow through vertical plate in the presence of Hall current (2019) Springer Nature Switzerland.
https://doi.org/10.1007/s42452-019-1656-0

Chambre PL, Young JD (1958) On the diffusion of a chemically reactive species in a laminar boundary layer. Phys Fluids 1:48–54
https://doi.org/10.1063/1.1724336

Cussler EL (1998) Diffusion mass transfer in fluid systems. Cambridge University Press, London
www.cambridge.org/9780521871211

Das UN, Deka RK, Soundalgekar VM (1994) Effects of mass transfer on flow past an impulsively started infinite vertical plate with constant heat flux and chemical reaction. Forsch Ingenieurwes 60:284–287
https://doi.org/10.1007/BF02601318

Ghosh SK, Bég OA (2008) Theoretical analysis of radiativeeffects on transient free convection heat transfer past a hot vertical surface in porous media. Nonlinear Anal Model Control 13(4):419–432
https://doi.org/10.15388/NA.2008.13.4.14548

Hari R. Kataria , Harshad R Patel(2016) Soret and heat generation effects on MHD Casson fluid flow past an oscillating vertical plate embedded through porous medium. Alexandria Engineering Journal 1-13.
https://doi.org/10.1016/j.aej.2016.06.024

Haroon Ur Rasheed , Saeed Islam, Zeeshan and Waris Khan,Jahangir Khan and Tariq Abbas (2022) Numerical modeling of unsteady MHD flow of Casson fluid in a vertical surface with chemical reaction and Hall current. Advances in Mechanical Engineering:1-10
https://doi.org/10.1177/16878132221085429

Nield DA, Bejan A (1999) Convection in porous media, 2nd edn. Springer, New York.
https://doi.org/10.1007/978-1-4614-5541-7

Postelnicu A (2007) Influence of chemical reaction on heat and mass by natural convection from vertical surfaces in porous media considering Soret and Dufour effects. Heat Mass Transf 43:595–602
10.1007/s00231-006-0132-8

Prased KV, Abdel S, Dahi PS (2003) Diffusion of chemically reactive species of a non-Newtonian fluid immersed in a porous medium over a stretching sheet. Int J Non-Linear Mech 3:651–657
https://doi.org/10.1016/j.jmaa.2005.06.095

R.A. Mohamed · Abdel-Nasser A. Osman ·S.M. Abo-Dahab(2013) Unsteady MHD double-diffusive convection boundary-layer flow past a radiate hot vertical surface in porous media in the presence of chemical reaction and heat sink Meccanica (2013) 48:931–942
https://doi.org/10.1007/s11012-012-9644-0

Raptis A, Perdikis C (2004) Unsteady flow through a highly porous medium in the presence of radiation. Transp Porous Media 57(2):171–179
https://doi.org/10.1023/B:TIPM.0000038262.65594.e8

Vijaya N, Arifuzzaman S M, Raghavendra Sai N, Manikya Rao Ch (2020) analysis of arrhenius activation energy in electrically conducting casson fluid flow induced due to permeable elongated sheet with chemical reaction and viscous dissipation. Frontiers in Heat and Mass Transfer, 15(26) (2020), 1-9
http://dx.doi.org/10.5098/hmt.15.26

Talha Anwar, Poom Kumam, and Wiboonsak Watthayu (2021) Unsteady MHD natural convection flow of Casson fluid incorporating thermal radiative flux and heat injection/suction mechanism under variable wall conditions. Scientific reports
https://doi.org/10.1038/s41598-021-83691-2

Vijaya N, Krishna Jyothi P , Anupamac A , Leelavathi R, Ambica K (2021) Thermophoresis and buoyancy effects on chemically reactive upper convected maxwell fluid flow induced by an exponentially stretching sheet: application of cattaneo-christov heat flux. Frontiers in Heat and Mass Transfer, 17(23) (2021), 1-8
http://dx.doi.org/10.5098/hmt.17.23

Frontiers in Heat and Mass Transfer (FHMT), 19, 36 (2022) Global Digital Central
DOI: 10.5098/hmt.19.36 ISSN: 2151-8629

APPENDIX

$A = 1 + \frac{1}{\beta}, \frac{Gr}{A} = B_1, \frac{Gm}{A} = B_2,$

$B_3 = \frac{1}{1 + \frac{1}{\beta}}, M^2 + k_p{}^2 = B_4, B_5 = \frac{Pr}{1 + R}$

$A_1 = -scsrB_5,\ A_2 = B_5 - Sc,$

$A3 = B_5 Q - Sckr,$

$A_4 = \frac{A_1}{A_2}, A_5 = \frac{A_3}{A_2}, A_6 = \frac{Q}{A_5}$

$A_7 = \frac{A_5 - Q}{A_5}, A_8 = -A_4 A_6,$

$A_9 = -A_4 A_7, A_{10} = A_5 - Q$

$A_{11} = A_5 - kr,\ A_{12} = B_5 - 1,$

$A_{13} = B_5 Q - B_4, \mathbf{A}_{14} = \frac{A_{13}}{A_{12}},$

$\mathbf{A}_{15} = \frac{Gr}{A_{12}}, \mathbf{A}_{16} = \frac{A_{15}}{A_{14}},$

$A_{17} = sckr - B_4, A_{18} = B_5 Q - B_4$

$A_{19} = Sc - 1, A_{20} = B_5 - 1,$

$\mathbf{A}_{21} = \frac{A_{17}}{A_{19}}, A_{22} = \frac{A_{18}}{A_{20}}$